3-2018

Observation of Ξc(2930)0 and updated measurement of B−→K−Λ+cΛ¯−c at Belle

Y. B. Li et al.
Belle Collaboration

Ratnappuli L. Kulasiri
Kennesaw State University, rkulasir@kennesaw.edu

Recommended Citation
Li, Y.B., Shen, C.P., Adachi, I. et al. Eur. Phys. J. C (2018) 78: 252. https://doi.org/10.1140/epjc/s10052-018-5720-5

Eur. Phys. J. C (2018) 78:252
https://doi.org/10.1140/epjc/s10052-018-5720-5

THE EUROPEAN PHYSICAL JOURNAL C

CrossMark

Regular Article - Experimental Physics

Observation of $\Xi_c(2930)^0$ and updated measurement of $B^- \to K^- \Lambda_c^+ \bar{\Lambda}_c^-$ at Belle

Belle Collaboration

Y. B. Li[65], C. P. Shen[2,a], I. Adachi[11,15], J. K. Ahn[38], H. Aihara[79], S. Al Said[36,73], D. M. Asner[63], T. Aushev[52], R. Ayad[73], V. Babu[74], I. Badhrees[35,73], A. M. Bakich[72], Y. Ban[65], V. Bansal[63], P. Behera[22], M. Berger[70], V. Bhardwaj[18], B. Bhuyan[20], J. Biswal[31], G. Bonvicini[84], A. Bozek[59], M. Bračko[31,47], T. E. Browder[14], D. Červenkov[4], V. Chekelian[48], A. Chen[56], B. G. Cheon[13], K. Chilikin[42,51], K. Cho[37], S.-K. Choi[12], Y. Choi[71], D. Cinabro[84], S. Cunliffe[63], N. Dash[19], S. Di Carlo[84], Z. Doležal[4], Z. Drásal[4], S. Eidelman[3,61], D. Epifanov[3,61], J. E. Fast[63], T. Ferber[7], B. G. Fulsom[63], R. Garg[64], V. Gaur[83], N. Gabyshev[3,61], A. Garmash[3,61], M. Gelb[33], A. Giri[21], P. Goldenzweig[33], E. Guido[29], J. Haba[11,15], T. Hara[11,15], K. Hayasaka[60], H. Hayashii[55], M. T. Hedges[14], W.-S. Hou[58], T. Iijima[53,54], K. Inami[53], G. Inguglia[7], A. Ishikawa[77], R. Itoh[11,15], M. Iwasaki[62], Y. Iwasaki[15], W. W. Jacobs[23], S. Jia[2], Y. Jin[79], K. K. Joo[5], T. Julius[49], G. Karyan[7], Y. Kato[53], T. Kawasaki[60], H. Kichimi[15], C. Kiesling[48], D. Y. Kim[69], J. B. Kim[38], K. T. Kim[38], S. H. Kim[13], K. Kinoshita[6], P. Kodyš[4], S. Korpar[31,47], D. Kotchetkov[14], P. Križan[31,43], R. Kroeger[27], P. Krokovny[3,61], R. Kulasiri[34], T. Kumita[81], A. Kuzmin[3,61], Y.-J. Kwon[85], I. S. Lee[13], S. C. Lee[40], L. K. Li[24], L. Li Gioi[48], J. Libby[22], D. Liventsev[15,83], M. Lubej[31], T. Luo[9], J. MacNaughton[15], M. Masuda[78], T. Matsuda[50], M. Merola[28], K. Miyabayashi[55], H. Miyata[60], R. Mizuk[42,51,52], G. B. Mohanty[74], H. K. Moon[38], T. Mori[53], M. Mrvar[31], R. Mussa[29], E. Nakano[62], M. Nakao[11,15], T. Nanut[31], K. J. Nath[20], Z. Natkaniec[59], M. Nayak[15,84], M. Niiyama[39], S. Nishida[11,15], S. Ogawa[76], P. Pakhlov[42,51], G. Pakhlova[42,52], B. Pal[6], S. Pardi[28], C. W. Park[71], H. Park[40], S. Paul[75], T. K. Pedlar[45], R. Pestotnik[31], L. E. Piilonen[83], V. Popov[52], A. Rostomyan[7], G. Russo[28], Y. Sakai[11,15], M. Salehi[44,46], S. Sandilya[6], L. Santelj[15], T. Sanuki[77], O. Schneider[41], G. Schnell[1,17], C. Schwanda[25], Y. Seino[60], V. Shebalin[3,61], T.-A. Shibata[80], J.-G. Shiu[58], B. Shwartz[3,61], A. Sokolov[26], E. Solovieva[42,52], M. Starič[31], J. F. Strube[63], M. Sumihama[10], T. Sumiyoshi[81], M. Takizawa[16,66,68], U. Tamponi[29,82], K. Tanida[30], F. Tenchini[49], M. Uchida[80], T. Uglov[42,52], Y. Unno[13], S. Uno[11,15], C. Van Hulse[1], G. Varner[14], V. Vorobyev[3,61], A. Vossen[23], E. Waheed[49], B. Wang[6], C. H. Wang[57], M.-Z. Wang[58], P. Wang[24], X. L. Wang[9], M. Watanabe[60], Y. Watanabe[32], E. Widmann[70], E. Won[38], H. Ye[7], J. Yelton[8], C. Z. Yuan[24], Y. Yusa[60], S. Zakharov[42,52], Z. P. Zhang[67], V. Zhilich[3,61], V. Zhukova[42,51], V. Zhulanov[3,61]

[1] University of the Basque Country UPV/EHU, 48080 Bilbao, Spain
[2] Beihang University, Beijing 100191, China
[3] Budker Institute of Nuclear Physics SB RAS, Novosibirsk 630090, Russia
[4] Faculty of Mathematics and Physics, Charles University, 121 16 Prague, Czech Republic
[5] Chonnam National University, Kwangju 660-701, South Korea
[6] University of Cincinnati, Cincinnati, OH 45221, USA
[7] Deutsches Elektronen-Synchrotron, 22607 Hamburg, Germany
[8] University of Florida, Gainesville, FL 32611, USA
[9] Fudan University, Shanghai 200443, China
[10] Gifu University, Gifu 501-1193, Japan
[11] SOKENDAI (The Graduate University for Advanced Studies), Hayama 240-0193, Japan
[12] Gyeongsang National University, Chinju 660-701, South Korea
[13] Hanyang University, Seoul 133-791, South Korea
[14] University of Hawaii, Honolulu, HI 96822, USA
[15] High Energy Accelerator Research Organization (KEK), Tsukuba 305-0801, Japan
[16] J-PARC Branch, KEK Theory Center, High Energy Accelerator Research Organization (KEK), Tsukuba 305-0801, Japan
[17] IKERBASQUE, Basque Foundation for Science, 48013 Bilbao, Spain
[18] Indian Institute of Science Education and Research Mohali, SAS Nagar 140306, India
[19] Indian Institute of Technology Bhubaneswar, Satya Nagar, Bhubaneswar 751007, India
[20] Indian Institute of Technology Guwahati, Guwahati, Assam 781039, India
[21] Indian Institute of Technology Hyderabad, Sangareddy, Telangana 502285, India
[22] Indian Institute of Technology Madras, Chennai 600036, India
[23] Indiana University, Bloomington, IN 47408, USA
[24] Institute of High Energy Physics, Chinese Academy of Sciences, Beijing 100049, China

[25] Institute of High Energy Physics, 1050 Vienna, Austria
[26] Institute for High Energy Physics, Protvino 142281, Russia
[27] University of Mississippi, University, MS 38677, USA
[28] INFN-Sezione di Napoli, 80126 Naples, Italy
[29] INFN-Sezione di Torino, 10125 Turin, Italy
[30] Advanced Science Research Center, Japan Atomic Energy Agency, Naka 319-1195, Japan
[31] J. Stefan Institute, 1000 Ljubljana, Slovenia
[32] Kanagawa University, Yokohama 221-8686, Japan
[33] Institut für Experimentelle Kernphysik, Karlsruher Institut für Technologie, 76131 Karlsruhe, Germany
[34] Kennesaw State University, Kennesaw 30144, Georgia
[35] King Abdulaziz City for Science and Technology, Riyadh 11442, Saudi Arabia
[36] Department of Physics, Faculty of Science, King Abdulaziz University, Jeddah 21589, Saudi Arabia
[37] Korea Institute of Science and Technology Information, Daejeon 305-806, South Korea
[38] Korea University, Seoul 136-713, South Korea
[39] Kyoto University, Kyoto 606-8502, Japan
[40] Kyungpook National University, Daegu 702-701, South Korea
[41] École Polytechnique Fédérale de Lausanne (EPFL), 1015 Lausanne, Switzerland
[42] P.N. Lebedev Physical Institute of the Russian Academy of Sciences, Moscow 119991, Russia
[43] Faculty of Mathematics and Physics, University of Ljubljana, 1000 Ljubljana, Slovenia
[44] Ludwig Maximilians University, 80539 Munich, Germany
[45] Luther College, Decorah, IA 52101, USA
[46] University of Malaya, 50603 Kuala Lumpur, Malaysia
[47] University of Maribor, 2000 Maribor, Slovenia
[48] Max-Planck-Institut für Physik, 80805 Munich, Germany
[49] School of Physics, University of Melbourne, Melbourne, VIC 3010, Australia
[50] University of Miyazaki, Miyazaki 889-2192, Japan
[51] Moscow Physical Engineering Institute, Moscow 115409, Russia
[52] Moscow Institute of Physics and Technology, Moscow, Moscow Region 141700, Russia
[53] Graduate School of Science, Nagoya University, Nagoya 464-8602, Japan
[54] Kobayashi-Maskawa Institute, Nagoya University, Nagoya 464-8602, Japan
[55] Nara Women's University, Nara 630-8506, Japan
[56] National Central University, Chung-li 32054, Taiwan
[57] National United University, Miao Li 36003, Taiwan
[58] Department of Physics, National Taiwan University, Taipei 10617, Taiwan
[59] H. Niewodniczanski Institute of Nuclear Physics, 31-342 Kraków, Poland
[60] Niigata University, Niigata 950-2181, Japan
[61] Novosibirsk State University, Novosibirsk 630090, Russia
[62] Osaka City University, Osaka 558-8585, Japan
[63] Pacific Northwest National Laboratory, Richland, WA 99352, USA
[64] Panjab University, Chandigarh 160014, India
[65] Peking University, Beijing 100871, China
[66] Theoretical Research Division, Nishina Center, RIKEN, Saitama 351-0198, Japan
[67] University of Science and Technology of China, Hefei 230026, China
[68] Showa Pharmaceutical University, Tokyo 194-8543, China
[69] Soongsil University, Seoul 156-743, South Korea
[70] Stefan Meyer Institute for Subatomic Physics, 1090 Vienna, Austria
[71] Sungkyunkwan University, Suwon 440-746, South Korea
[72] School of Physics, University of Sydney, Sydney, NSW 2006, Australia
[73] Department of Physics, Faculty of Science, University of Tabuk, Tabuk 71451, Saudi Arabia
[74] Tata Institute of Fundamental Research, Mumbai 400005, India
[75] Department of Physics, Technische Universität München, 85748 Garching, Germany
[76] Toho University, Funabashi 274-8510, Japan
[77] Department of Physics, Tohoku University, Sendai 980-8578, Japan
[78] Earthquake Research Institute, University of Tokyo, Tokyo 113-0032, Japan
[79] Department of Physics, University of Tokyo, Tokyo 113-0033, Japan
[80] Tokyo Institute of Technology, Tokyo 152-8550, Japan
[81] Tokyo Metropolitan University, Tokyo 192-0397, Japan
[82] University of Torino, 10124 Turin, Italy
[83] Virginia Polytechnic Institute and State University, Blacksburg, VA 24061, USA
[84] Wayne State University, Detroit, MI 48202, USA
[85] Yonsei University, Seoul 120-749, South Korea

Received: 25 January 2018 / Accepted: 8 March 2018 / Published online: 23 March 2018

Abstract We report the first observation of the $\Xi_c(2930)^0$ charmed-strange baryon with a significance greater than 5σ. The $\Xi_c(2930)^0$ is found in its decay to $K^-\Lambda_c^+$ in $B^- \to K^-\Lambda_c^+\bar{\Lambda}_c^-$ decays. The measured mass and width are $[2928.9 \pm 3.0(\text{stat.})^{+0.9}_{-12.0}(\text{syst.})]$ MeV/c^2 and $[19.5 \pm 8.4(\text{stat.})^{+5.9}_{-7.9}(\text{syst.})]$ MeV, respectively, and the product branching fraction is $\mathcal{B}(B^- \to \Xi_c(2930)^0\bar{\Lambda}_c^-)\mathcal{B}(\Xi_c(2930)^0 \to K^-\Lambda_c^+) = [1.73 \pm 0.45(\text{stat.}) \pm 0.21(\text{syst.})] \times 10^{-4}$. We also measure $\mathcal{B}(B^- \to K^-\Lambda_c^+\bar{\Lambda}_c^-) = [4.80 \pm 0.43(\text{stat.}) \pm 0.60(\text{syst.})] \times 10^{-4}$ with improved precision, and search for the charmonium-like state $Y(4660)$ and its spin partner, Y_η, in the $\Lambda_c^+\bar{\Lambda}_c^-$ invariant mass spectrum. No clear signals of the $Y(4660)$ nor its spin partner are observed and the 90% credibility level (C.L.) upper limits on their production rates are determined. These measurements are obtained from a sample of $(772 \pm 11) \times 10^6 B\bar{B}$ pairs collected at the $\Upsilon(4S)$ resonance by the Belle detector at the KEKB asymmetric energy electron–positron collider.

The singly charmed baryon is composed of a charm quark and two light quarks. Charmed baryon spectroscopy provides an excellent ground for studying the dynamics of light quarks in the environment of a heavy quark and offers an excellent laboratory for testing heavy-quark or chiral symmetry of the heavy or light quarks, respectively. Although many new excited charmed baryons have been discovered by BaBar, Belle, CLEO and LHCb in the past two decades [1], and many efforts have been made to identify the quantum numbers of these new states and understand their properties, we do not yet have a fully phenomenological model that describes the complicated physics of this sector [2,3]. Identification and observation of new members in the charmed-baryon family will provide more information to address these open issues.

The $\Xi_c(2930)$ charmed-strange baryon has been reported only in the analysis of $B^- \to K^-\Lambda_c^+\bar{\Lambda}_c^-$ by BaBar [4], where they claim a signal in the $K^-\Lambda_c^+$ invariant mass distribution with a mass of $[2931 \pm 3(\text{stat.}) \pm 5(\text{syst.})]$ MeV/c^2 and a width of $[36 \pm 7(\text{stat.}) \pm 11(\text{syst.})]$ MeV. However, neither the results of the fit to their spectrum nor the significance of the signal were given; the Particle Data Group (PDG) lists it as a "one star" state [1]. Despite the weak experimental evidence for the $\Xi_c(2930)$ state, it has been taken into account in many theoretical models, including the chiral quark model [5], the light-cone Quantum Chromodynamics (QCD) sum rule [6], the $^3P_0$ mode [7], the constituent quark model [8,9], and the heavy-hadron chiral perturbation theory [10].

Belle has previously studied $B^- \to K^-\Lambda_c^+\bar{\Lambda}_c^-$ decays [11] with a data sample of 386×10^6 $B\bar{B}$ pairs but the distributions of the intermediate $K\Lambda_c$ systems have not been presented. The full Belle data sample of $(772 \pm 11) \times 10^6 B\bar{B}$ pairs permits an improved study of $B^- \to K^-\Lambda_c^+\bar{\Lambda}_c^-$ and a test for the existence of the $\Xi_c(2930)$.

The same B decay mode can be used to study the $\Lambda_c^+\bar{\Lambda}_c^-$ invariant mass. In this system, Belle has previously observed a charmonium-like state, the $Y(4630)$, in the initial state radiation (ISR) process $e^+e^- \to \gamma_{\text{ISR}}\Lambda_c^+\bar{\Lambda}_c^-$ [12] with a measured mass of $[4634^{+8}_{-7}(\text{stat.})^{+5}_{-8}(\text{syst.})]$ MeV/c^2 and a width of $[92^{+40}_{-24}(\text{stat.})^{+10}_{-21}(\text{syst.})]$ MeV. As this mass is very close to that of the $Y(4660)$ observed by Belle in the ISR process $e^+e^- \to \gamma_{\text{ISR}}\pi^+\pi^-\psi'$ [13,14], many theoretical explanations assume they are the same state [15–17]. In Refs. [18,19], where the $Y(4660)$ is modeled as an $f_0(980)\psi'$ bound state, the authors predict that it should have a spin partner—a $f_0(980)\eta_c(2S)$ bound state denoted as the Y_η—with a mass and width of (4613 ± 4) MeV/c^2 and around 30 MeV, respectively, and a large partial width into $\Lambda_c^+\bar{\Lambda}_c^-$ [17,19].

In this Letter, we perform an updated measurement of $B^- \to K^-\Lambda_c^+\bar{\Lambda}_c^-$ [20] and observe the $\Xi_c(2930)^0$ signal with a significance of 5.1σ. This analysis is based on the full data sample collected at the $\Upsilon(4S)$ resonance by the Belle detector [21,22] at the KEKB asymmetric energy electron–positron collider [23,24]. Simulated signal events with B meson decays are generated using EvtGen [25], while the inclusive decays are generated via PYTHIA [26]. These events are processed by a detector simulation based on GEANT3 [27]. Inclusive Monte Carlo (MC) samples of $\Upsilon(4S) \to B\bar{B}$ ($B = B^+$ or B^0) and $e^+e^- \to q\bar{q}$ ($q = u,\ d,\ s,\ c$) events at $\sqrt{s} = 10.58$ GeV are used to check the backgrounds, corresponding to more than 5 times the integrated luminosity of the data.

We reconstruct the Λ_c^+ via the $\Lambda_c^+ \to pK^-\pi^+$, pK_S^0, $\Lambda\pi^+$, $pK_S^0\pi^+\pi^-$, and $\Lambda\pi^+\pi^+\pi^-$ decay channels. When a Λ_c^+ and $\bar{\Lambda}_c^-$ are combined to reconstruct a B candidate, at least one is required to have been reconstructed via the $pK^+\pi^-$ or $\bar{p}K^-\pi^+$ decay process. For charged tracks, information from different detector subsystems, including specific ionization in the central drift chamber, time measurements in the time-of-flight scintillation counters and the response of the aerogel threshold Cherenkov counters, is combined to form the likelihood $\mathcal{L}_i$ for species i, where $i = \pi$, K, or p [28]. Except for the charged tracks from $\Lambda \to p\pi^-$ and $K_S^0 \to \pi^+\pi^-$ decays, a track with a likelihood ratio $\mathcal{R}_K^\pi = \mathcal{L}_K/(\mathcal{L}_K + \mathcal{L}_\pi) > 0.6$ is identified as a kaon, while a track with $\mathcal{R}_K^\pi < 0.4$ is treated as a pion [28]. With this selection, the kaon (pion) identification efficiency is about 94% (98%), while 5% (2%) of the kaons (pions) are misidentified as pions (kaons). A track with $\mathcal{R}_{p/\bar{p}}^\pi = \mathcal{L}_{p/\bar{p}}/(\mathcal{L}_{p/\bar{p}} + \mathcal{L}_\pi) > 0.6$ and $\mathcal{R}_{p/\bar{p}}^K = \mathcal{L}_{p/\bar{p}}/(\mathcal{L}_{p/\bar{p}} + \mathcal{L}_K) > 0.6$ is identified as a proton/anti-proton with an efficiency of about 98%; fewer than 1% of the pions/kaons are misidentified as protons/anti-protons.

[a] e-mail: shencp@phys.hawaii.edu

The K_S^0 candidates are reconstructed from pairs of oppositely-charged tracks, treated as pions, and identified by a multivariate analysis with a neural network [29] based on two sets of input variables [30]. Candidate Λ baryons are reconstructed in the decay $\Lambda \to p\pi^-$ and selected if the $p\pi^-$ invariant mass is within 5 MeV/c^2 (5σ) of the Λ nominal mass [1].

We perform a vertex fit to signal B candidates. If there is more than one B signal candidate in an event, we select the one with the minimum $\chi^2_{\rm vertex}$ from the vertex fit. We require $\chi^2_{\rm vertex} < 50$ with a selection efficiency above 96%. As the continuum background level is very low, continuum suppression is not necessary.

The B candidates are identified using the beam-energy constrained mass $M_{\rm bc}$ and the mass difference ΔM_B. The beam-energy constrained mass is defined as $M_{\rm bc} \equiv \sqrt{E^2_{\rm beam}/c^2 - (\sum \vec{p}_i)^2}/c$, where $E_{\rm beam}$ is the beam energy and $\vec{p}_i$ are the three-momenta of the B-meson decay products, all defined in the center-of-mass system (CMS) of the e^+e^- collision. The mass difference is defined as $\Delta M_B \equiv M_B - m_B$, where M_B is the invariant mass of the B candidate and m_B is the nominal B-meson mass [1].

Figure 1 shows clear evidence of Λ_c^+ and $\bar{\Lambda}_c^-$ in the distribution of $M_{\bar{\Lambda}_c^-}$ versus $M_{\Lambda_c^+}$ (left panel) from the selected $B^- \to K^-\Lambda_c^+\bar{\Lambda}_c^-$ data candidates in the B signal region of $|\Delta M_B| < 0.018\,{\rm GeV}/c^2$ and $M_{\rm bc} > 5.27\,{\rm GeV}/c^2$ ($\sim 3\sigma$), illustrated by the green box in the right panel's distribution of ΔM_B versus $M_{\rm bc}$. The Λ_c signal region (the central green box in the left panel) is defined as $|M_{\Lambda_c} - m_{\Lambda_c}| < 10$ MeV/c^2 ($\sim 2.5\sigma$), where m_{Λ_c} is the nominal mass of the Λ_c baryon [1]. As the mass resolution of Λ_c candidates is almost independent of the Λ_c decay mode, according to the signal MC simulation, the same requirement is placed on all Λ_c decay modes. The non-Λ_c background in the Λ_c signal region is estimated as half of the total number of events in the four red sideband regions minus one quarter of the total number of events in the four blue sideband regions of the left panel.

To obtain the $B^- \to K^-\Lambda_c^+\bar{\Lambda}_c^-$ signal yields, we perform an unbinned two-dimensional (2D) simultaneous extended maximum likelihood fit to the ΔM_B versus $M_{\rm bc}$ distributions for the five reconstructed Λ_c decay modes. The model used to fit the $M_{\rm bc}$ distribution is a Gaussian function for the signal shape plus an ARGUS function [31] for the background. The model for the ΔM_B distribution is the sum of a Gaussian function for the signal plus a first-order polynomial for the background. The Gaussian resolutions are fixed to the values from the fits to the individual MC distributions, and the relative signal yields among the five final states is fixed according to the relative branching fraction between the final states and the detection acceptance and efficiency of the intermediate states.

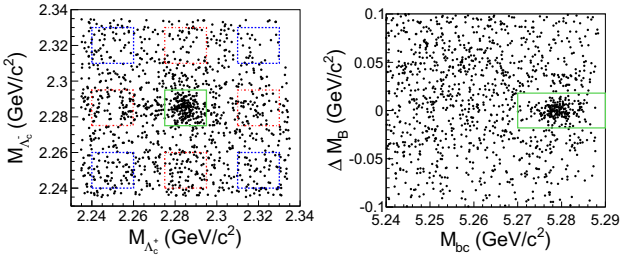

Fig. 1 Signal-enhanced distribution of $M(\bar{\Lambda}_c^-)$ versus $M(\Lambda_c^+)$ (left panel) and of ΔM_B versus $M_{\rm bc}$ (right panel) from the selected $B^- \to K^-\Lambda_c^+\bar{\Lambda}_c^-$ candidates, summing over all five reconstructed Λ_c decay modes. Each panel shows the events falling in the solid green signal region of the other panel. The dashed red and blue boxes in the left panel show the Λ_c sideband regions used for the estimation of the non-Λ_c background (see text)

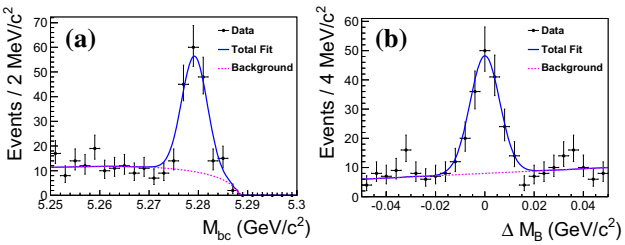

Fig. 2 The Λ_c-signal-enhanced distributions of (a) $M_{\rm bc}$ in the ΔM_B signal region and (b) ΔM_B in the $M_{\rm bc}$ signal region for $B^- \to K^-\Lambda_c^+\bar{\Lambda}_c^-$, combining five exclusive final states. The dots with error bars are data, the solid blue curves are the best-fit projections to the distributions and the dashed magenta lines are the fitted backgrounds

Figure 2 shows the projections of the fit superimposed on the Λ_c-signal-enhanced $M_{\rm bc}$ and ΔM_B distributions, summing over all five reconstructed Λ_c decay modes. We observe 153 ± 14 signal events with a signal significance above 10σ, and extract the branching fraction of $\mathcal{B}(B^- \to K^-\Lambda_c^+\bar{\Lambda}_c^-) = [4.80 \pm 0.43({\rm stat.})] \times 10^{-4}$.

The Dalitz distribution of the reconstructed $B^- \to K^-\Lambda_c^+\bar{\Lambda}_c^-$ candidates is shown in Fig. 3. A vertical-band enhancement near $M(K^-\Lambda_c^+) \sim 2.93$ GeV/c^2 is observed; no signal band is apparent in the $M(\Lambda_c^+\bar{\Lambda}_c^-)$ horizontal direction nor in the $M(K^-\bar{\Lambda}_c^-)$ diagonal direction.

The B-signal-enhanced $K^-\Lambda_c^+$ mass spectrum is shown in Fig. 4. The shaded histogram is from the normalized Λ_c^+ and $\bar{\Lambda}_c^-$ mass sidebands, and the dot-dashed line is the sum of the contributions from normalized $e^+e^- \to q\bar{q}$ and $\Upsilon(4S) \to B\bar{B}$ generic MC samples. Since they are consistent, we take the Λ_c^+ and $\bar{\Lambda}_c^-$ mass sidebands to represent the total background, neglecting the small possible contribution of background with real Λ_c^+ and $\bar{\Lambda}_c^-$. A clear $\Xi_c(2930)$ signal is observed. No structure is seen in the Λ_c^+ and $\bar{\Lambda}_c^-$ mass sidebands, nor in the generic MC samples, nor in the wrong-sign-combination distribution of $K^-\bar{\Lambda}_c^-$.

An unbinned simultaneous extended maximum likelihood fit is performed to the $K^-\Lambda_c^+$ invariant mass spectra for

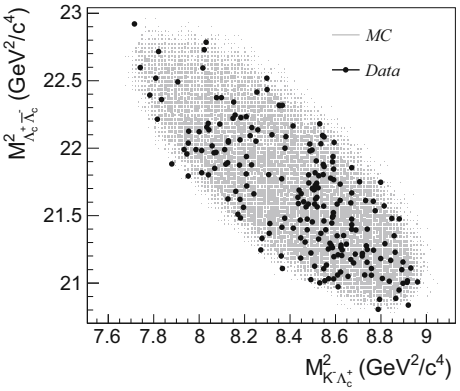

Fig. 3 Dalitz distribution of reconstructed $B^- \to K^-\Lambda_c^+\bar{\Lambda}_c^-$ candidates in the B signal region. The black dots are data; the shaded region is the MC simulated phase-space distribution

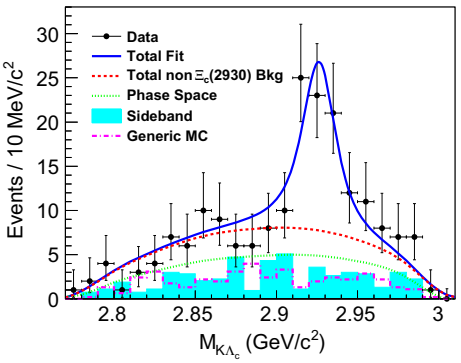

Fig. 4 The $M_{K^-\Lambda_c^+}$ distribution of the selected data candidates, with fit results superimposed. Dots with error bars are the data, the solid blue line is the best fit, the dashed red line is the total non-$\Xi_c(2930)$ backgrounds, the dotted green line is the phase space contribution, the shaded cyan histogram is from the normalized Λ_c^+ and $\bar{\Lambda}_c^-$ mass sidebands, and the dot-dashed magenta line is the sum of the MC-simulated contributions from the normalized $e^+e^- \to q\bar{q}$ and $\Upsilon(4S) \to B\bar{B}$ generic-decay backgrounds

selected B- and Λ_c-signal events and the Λ_c^+ and $\bar{\Lambda}_c^-$ mass sidebands. An S-wave Breit-Wigner (BW) function convolved with a Gaussian function with the phase space factor and efficiency curve included (the mass resolution of Gaussian function being fixed to 4.46 MeV/c^2 from the signal MC simulation) is taken as the $\Xi_c(2930)$ signal shape. Direct three-body B decays are modeled by the shape corresponding to $B^- \to K^-\Lambda_c^+\bar{\Lambda}_c^-$ MC-simulated decays distributed uniformly in phase space. A second-order polynomial is used to represent the Λ_c^+ and $\bar{\Lambda}_c^-$ mass-sideband distribution, which is normalized to represent the total background in the signal events in the fit.

The fit results are shown in Fig. 4. The fitted mass and width of the $\Xi_c(2930)$ are $M_{\Xi_c(2930)} = [2928.9 \pm 3.0(\text{stat.})]$ MeV/c^2 and $\Gamma_{\Xi_c(2930)} = [19.5 \pm 8.4(\text{stat.})]$ MeV, where a fit bias of 1.4 MeV/c^2 on the $\Xi_c(2930)$ mass, determined using MC simulation, has been corrected. The yields of the $\Xi_c(2930)$ signal and the phase-space contribution are $N_{\Xi_c} = 61 \pm 16$ and $N_{\text{phsp}} = 79 \pm 19$.

To estimate the $\Xi_c(2930)$ signal significance, we use an ensemble of simulated experiments to estimate the probability that background fluctuations alone would produce signals as significant as that seen in the data. We generate $K^-\Lambda_c^+$ mass spectra according to the shape of the non-$\Xi_c(2930)$ background distribution (the dashed red line in Fig. 4), with each spectrum containing 192 events which corresponds to the total data entries in Fig. 4. We fit each spectrum as we do the real data, searching for the most significant fluctuation, and thus obtain the distribution of $-2\ln(L_0/L_{\max})$ for these simulated background samples. We perform a total of 13.2 million simulations and found 3 trials with a $-2\ln(L_0/L_{\max})$ value greater than or equal to the value obtained in the data. The resulting p value is 2.27×10^{-7}, corresponding to a significance of 5.1σ.

The product branching fraction of $\mathcal{B}(B^- \to \Xi_c(2930)\bar{\Lambda}_c^-)\mathcal{B}(\Xi_c(2930) \to K^-\Lambda_c^+) = [1.73 \pm 0.45(\text{stat.})] \times 10^{-4}$ is calculated as $N^{\Xi_c}_{\text{total}}/[2N_{B^\pm}\varepsilon^{\Xi_c}_{\text{all}}\mathcal{B}(\Lambda_c^+ \to pK^-\pi^+)^2]$, where $N^{\Xi_c}_{\text{total}}$ is the fitted $\Xi_c(2930)$ signal yield; $N_{B^\pm} = N_{\Upsilon(4S)}\mathcal{B}(\Upsilon(4S) \to B^+B^-)$ ($N_{\Upsilon(4S)}$ is the number of accumulated $\Upsilon(4S)$ events and $\mathcal{B}(\Upsilon(4S) \to B^+B^-) = 0.514 \pm 0.006$ [1]); $\mathcal{B}(\Lambda_c^+ \to pK^-\pi^+) = (6.35 \pm 0.33)\%$ is the world-average branching fraction for $\Lambda_c^+ \to pK^-\pi^+$ [1]; $\varepsilon^{\Xi_c}_{\text{all}} = \sum \varepsilon_i^{\Xi_c} \times \Gamma_i/\Gamma(pK^-\pi^+)$ (i is the Λ_c decay-mode index, $\varepsilon_i^{\Xi_c}$ is the detection efficiency from MC simulation and Γ_i is the partial decay width of $\Lambda_c^+ \to pK^-\pi^+$, pK_S^0, $\Lambda\pi^-$, $pK_S^0\pi^+\pi^-$, and $\Lambda\pi^-\pi^+\pi^-$ [1]). Here, $\mathcal{B}(K_S^0 \to \pi^+\pi^-)$ or $\mathcal{B}(\Lambda \to p\pi^-)$ is included in Γ_i for the final states with a K_S^0 or a Λ.

The $M_{\Lambda_c^+\bar{\Lambda}_c^-}$ spectrum is shown in Fig. 5, in which no clear Y_η or $Y(4660)$ signals is evident. An unbinned extended maximum likelihood fit is applied to the $\Lambda_c^+\bar{\Lambda}_c^-$ mass spectrum to extract the signal yields of the Y_η and $Y(4660)$ in B decays. In the fit, the signal shape of the Y_η or $Y(4660)$ is obtained from MC simulation directly with the input parameters $M_{Y_\eta} = 4616$ MeV/c^2 and $\Gamma_{Y_\eta} = 30$ MeV for Y_η [17], and $M_{Y(4660)} = 4643$ MeV/c^2 and $\Gamma_{Y(4660)} = 72$ MeV for $Y(4660)$ [1]; a third-order polynomial is used to describe all other contributions. The fit results are shown in Figs. 5(a) and (b) for the Y_η and $Y(4660)$, respectively. From the fits, we have (10 ± 23) Y_η signal events with a statistical signal significance of 0.7σ, and (-10 ± 26) $Y(4660)$ signal events.

As the statistical signal significance of each Y state is less than 3σ, 90% C.L. Bayesian upper limits on $\mathcal{B}(B^- \to K^-Y)\mathcal{B}(Y \to \Lambda_c^+\bar{\Lambda}_c^-)$ are determined to be 1.2×10^{-4} and 2.0×10^{-4} for $Y = Y_\eta$ and $Y(4660)$, respectively, by solving the equation $\int_0^{\mathcal{B}^{\text{up}}} \mathcal{L}(\mathcal{B})d\mathcal{B}/\int_0^{+\infty} \mathcal{L}(\mathcal{B})d\mathcal{B} = 0.9$, where $\mathcal{B} = n_Y/[2\varepsilon^Y_{\text{all}}N_{B^\pm}\mathcal{B}(\Lambda_c^+ \to pK^-\pi^+)^2]$ is the assumed product branching fraction; $\mathcal{L}(\mathcal{B})$ is the corresponding max-

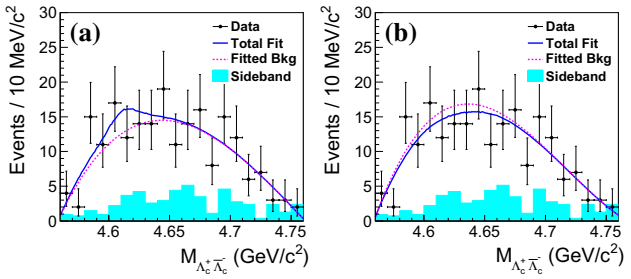

Fig. 5 The $\Lambda_c^+\bar{\Lambda}_c^-$ invariant mass spectra in data with (a) Y_η and (b) Y(4660) signals included in the fits. The solid blue lines are the best fits and the dotted red lines represent the backgrounds. The shaded cyan histograms are from the normalized Λ_c^+ and $\bar{\Lambda}_c^-$ mass sidebands

imized likelihood of the data; n_Y is the number of Y signal events; and $\varepsilon_{\rm all}^Y = \sum \varepsilon_i^Y \times \Gamma_i/\Gamma(pK^-\pi^+)$ (ε_i^Y being the total efficiency from MC simulation for mode i). To take the systematic uncertainty into account, the above likelihood is convolved with a Gaussian function whose width equals the total systematic uncertainty.

There are several sources of systematic uncertainties in the branching fraction measurements. The detection efficiency relevant (DER) errors include those for tracking efficiency (0.35%/track), particle identification efficiency (1.9%/kaon, 0.9%/pion, 2.4%/proton and 2.0%/anti-proton), as well as Λ (3.0%) and K_S^0 (1.7%) selection efficiencies. Assuming all the above systematic error sources are independent, the DER errors are summed in quadrature for each decay mode, yielding 5.8–8.3%, depending on the mode. For the four branching fraction measurements, the final DER errors are summed in quadrature over the five Λ_c decay modes using weight factors equal to the product of the total efficiency and the Λ_c partial decay width. We estimate the systematic errors associated with the fitting procedure by changing the order of the background polynomial, the range of the fit, and the values of the masses and widths of the Y_η and $Y(4660)$ by $\pm1\sigma$, and by enlarging the mass resolution by 10%; the deviations from nominal in the fitted results are taken as systematic errors. Uncertainties for $\mathcal{B}(\Lambda_c^+ \to pK^-\pi^+)$ and $\Gamma_i/\Gamma(pK^-\pi^+)$ are taken from Ref. [1]. The final errors on the Λ_c partial decay widths are summed in quadrature over the five modes with the detection efficiency as a weighting factor. The world average of $\mathcal{B}(\Upsilon(4S) \to B^+B^-)$ is $(51.4\pm0.6)\%$ [1], which corresponds to a systematic uncertainty of 1.2%. The systematic uncertainty on $N_{\Upsilon(4S)}$ is 1.37%. Assuming all sources listed in Table 1 to be independent, the total systematic uncertainties on the branching fraction measurements are summed in quadrature.

The following systematic uncertainties are considered for the $\Xi_c(2930)$ mass and width. Half of the correction due to the fitting bias on the $\Xi_c(2930)$ mass is taken conservatively as a systematic error. By enlarging the mass resolution by 10%, the difference in the measured $\Xi_c(2930)$ width is 0.7 MeV, which is taken as a systematic error. By changing the background shape, the differences of 0.3 MeV/c^2 and 0.9 MeV in the measured $\Xi_c(2930)$ mass and width, respectively, are taken as systematic uncertainties.

Table 1 Relative systematic uncertainties (%) in the branching fraction measurements. Here, $\mathcal{B}_1 \equiv \mathcal{B}(B^- \to K^-\Lambda_c^+\bar{\Lambda}_c^-)$, $\mathcal{B}_2 \equiv \mathcal{B}(B^- \to \Xi_c(2930)\bar{\Lambda}_c^-)\mathcal{B}(\Xi_c(2930) \to K^-\Lambda_c^+)$, $\mathcal{B}_3 \equiv \mathcal{B}(B^- \to K^-Y_\eta)\mathcal{B}(Y_\eta \to \Lambda_c^+\bar{\Lambda}_c^-)$, and $\mathcal{B}_4 \equiv \mathcal{B}(B^- \to K^-Y(4660))\mathcal{B}(Y(4660) \to \Lambda_c^+\bar{\Lambda}_c^-)$

Branching fraction	DER	Fit	Λ_c decays	$N_{B^\pm}$	Sum
$\mathcal{B}_1$	4.81	3.94	10.81	1.82	12.6
$\mathcal{B}_2$	4.73	2.27	10.81	1.82	12.1
$\mathcal{B}_3$	4.76	8.65	10.86	1.82	14.8
$\mathcal{B}_4$	4.77	23.1	10.83	1.82	26.0

The signal-parametrization systematic uncertainty is estimated by replacing the constant total width with a mass-dependent width of $\Gamma_t = \Gamma_t^0 \times \Phi(M_{K^-\Lambda_c^+})/\Phi(M_{\Xi_c(2930)})$, where Γ_t^0 is the width of the resonance, $\Phi(M_{K^-\Lambda_c^+}) = P/M_{K^-\Lambda_c^+}$ is the phase space factor for an S-wave two-body system (P is the K^- momentum in the $K^-\Lambda_c^+$ CMS) and $M_{\Xi_c(2930)}$ is the $K^-\Lambda_c^+$ invariant mass fixed at the $\Xi_c(2930)$ nominal mass. The differences in the measured $\Xi_c(2930)$ mass and width are 0.2 MeV/c^2 and 5.3 MeV, respectively, which are taken as the systematic errors. Adding an additional possible resonance with mass and width free at around 2.85 GeV/c^2 into the fit to the $M(K^-\Lambda_c^+)$ spectra, the fit gives $M_{\Xi_c(2930)} = (2929.3 \pm 3.1)$ MeV/c^2 and $\Gamma_{\Xi_c(2930)} = (21.7 \pm 9.3)$ MeV; the differences of $+0.4$ MeV/c^2 and $+2.2$ MeV from the mass and width found without the additional resonance, respectively, are taken as systematic errors. An alternative fit to the $M(K^-\Lambda_c^+)$ spectra with interference between the $\Xi_c(2930)$ and the phase-space contribution included gives $M_{\Xi_c(2930)} = (2917.0 \pm 5.5)$ MeV/c^2 and $\Gamma_{\Xi_c(2930)} = (13.8 \pm 6.9)$ MeV; the differences of -11.9 MeV/c^2 and -5.7 MeV from the nominal mass and width, respectively, are taken as systematic errors. Assuming all the sources are independent, we add them in quadrature to obtain the total systematic uncertainties on the $\Xi_c(2930)$ mass and width of $^{+0.9}_{-12.0}$ MeV/c^2 and $^{+5.9}_{-7.9}$ MeV, respectively.

In summary, using $(772 \pm 11) \times 10^6$ $B\bar{B}$ pairs, we perform an updated analysis of $B^- \to K^-\Lambda_c^+\bar{\Lambda}_c^-$. In the $K^-\Lambda_c^+$ mass spectrum, the charmed baryon state $\Xi_c(2930)^0$ is clearly observed for the first time with a statistical significance greater than 5σ. The measured mass and width are $M_{\Xi_c(2930)} = (2928.9 \pm 3.0^{+0.9}_{-12.0})$ MeV/c^2 and $\Gamma_{\Xi_c(2930)} = (19.5 \pm 8.4^{+5.9}_{-7.9})$ MeV. The branching fraction is $\mathcal{B}(B^- \to K^-\Lambda_c^+\bar{\Lambda}_c^-) = (4.80 \pm 0.43 \pm 0.60) \times 10^{-4}$, which is consistent with the world average value of $(6.9\pm2.2)\times10^{-4}$ [1] but with much-improved precision. We measure the product branching fraction $\mathcal{B}(B^- \to \Xi_c(2930)\bar{\Lambda}_c^-)\mathcal{B}(\Xi_c(2930) \to$

$K^-\Lambda_c^+) = (1.73 \pm 0.45 \pm 0.21) \times 10^{-4}$, where the first error is statistical and the second systematic. Because of the limited statistics, we do not attempt analysis of angular correlations to determine the spin parity of the $\Xi_c(2930)^0$, however we expect that this will be possible with the much larger data sample which will be collected with the Belle II detector. Without this information, we are not able to identify the quark content of this state as there are many theoretical possibilities. There are no significant signals seen in the $\Lambda_c^+\bar{\Lambda}_c^-$ mass spectrum. We place 90% C.L. upper limits for the $Y(4660)$ and its theoretically predicted spin partner Y_η of $\mathcal{B}(B^- \to K^-Y(4660))\mathcal{B}(Y(4660) \to \Lambda_c^+\bar{\Lambda}_c^-) < 1.2 \times 10^{-4}$ and $\mathcal{B}(B^- \to K^-Y_\eta)\mathcal{B}(Y_\eta \to \Lambda_c^+\bar{\Lambda}_c^-) < 2.0 \times 10^{-4}$ [32].

We thank the KEKB group for the excellent operation of the accelerator; the KEK cryogenics group for the efficient operation of the solenoid; and the KEK computer group, the National Institute of Informatics, and the PNNL/EMSL computing group for valuable computing and SINET5 network support. We acknowledge support from the Ministry of Education, Culture, Sports, Science, and Technology (MEXT) of Japan, the Japan Society for the Promotion of Science (JSPS), and the Tau-Lepton Physics Research Center of Nagoya University; the Australian Research Council; Austrian Science Fund under Grant No. P 26794-N20; the National Natural Science Foundation of China under Contracts No. 10575109, No. 10775142, No. 10875115, No. 11175187, No. 11475187, No. 11521505, No. 11575017 and No. 11761141009; the Chinese Academy of Science Center for Excellence in Particle Physics; Key Research Program of Frontier Sciences, Chinese Academy of Science, Grant No. QYZDJ-SSW-SLH011; the Ministry of Education, Youth and Sports of the Czech Republic under Contract No. LTT17020; the Carl Zeiss Foundation, the Deutsche Forschungsgemeinschaft, the Excellence Cluster Universe, and the VolkswagenStiftung; the Department of Science and Technology of India; the Istituto Nazionale di Fisica Nucleare of Italy; National Research Foundation (NRF) of Korea Grants No. 2014R1A2A2A01005286, No. 2015R1A2A2A01003280, No. 2015H1A2A1033649, No. 2016R1D1A1B01010135, No. 2016K1A3A7A09005603, No. 2016R1D1A1B02012900; Radiation Science Research Institute, Foreign Large-size Research Facility Application Supporting project and the Global Science Experimental Data Hub Center of the Korea Institute of Science and Technology Information; the Polish Ministry of Science and Higher Education and the National Science Center; the Ministry of Education and Science of the Russian Federation and the Russian Foundation for Basic Research; the Slovenian Research Agency; Ikerbasque, Basque Foundation for Science and MINECO (Juan de la Cierva), Spain; the Swiss National Science Foundation; the Ministry of Education and the Ministry of Science and Technology of Taiwan; and the U.S. Department of Energy and the National Science Foundation.

References

1. C. Patrignani et al. (Particle Data Group), Chin. Phys. C **40**, 100001 (2016) and 2017 update
2. V. Crede, W. Roberts, Rep. Prog. Phys. **76**, 076301 (2013)
3. H.Y. Cheng, Front. Phys. **10**, 101406 (2015)
4. B. Aubert et al. (BaBar Collaboration), Phys. Rev. D **77**, 031101 (2008)
5. L.H. Liu, L.Y. Xiao, X.H. Zhong, Phys. Rev. D **86**, 034024 (2012)
6. H.X. Chen, Q. Mao, W. Chen, A. Hosaku, X. Liu, S.L. Zhu, Phys. Rev. D **95**, 094008 (2017)
7. D.D. Ye, Z. Zhao, A.L. Zhang, Phys. Rev. D **96**, 114009 (2017)
8. K.L. Wang, Y.X. Yao, X.H. Zhong, Q. Zhao, Phys. Rev. D **96**, 116016 (2017)
9. B. Chen, K.W. Wei, X. Liu, T. Matsuki, Eur. Phys. J. C **77**, 154 (2017)
10. H.Y. Cheng, C.W. Chiang, Phys. Rev. D **95**, 094018 (2017)
11. N. Gabyshev et al. (Belle Collaboration), Phys. Rev. Lett. **97**, 202003 (2006)
12. G. Pakhlova et al. (Belle Collaboration), Phys. Rev. Lett. **101**, 172001 (2008)
13. X.L. Wang et al. (Belle Collaboration), Phys. Rev. Lett. **99**, 142002 (2007)
14. X.L. Wang et al. (Belle Collaboration), Phys. Rev. D **91**, 112007 (2015)
15. D.V. Bugg, J. Phys. G **36**, 075002 (2009)
16. G. Cotugno, R. Faccini, A.D. Polosa, C. Sabelli, Phys. Rev. Lett. **104**, 132005 (2010)
17. F.K. Guo, J. Haidenbauer, C. Hanhart, U.G. Meißner, Phys. Rev. D **82**, 094008 (2010)
18. F.K. Guo, C. Hanhart, U.G. Meißner, Phys. Lett. B **665**, 26 (2008)
19. F.K. Guo, C. Hanhart, U.G. Meißner, Phys. Rev. Lett. **102**, 242004 (2009)
20. Inclusion of charge conjugate states is implicit unless otherwise stated
21. A. Abashian et al. (Belle Collaboration), Nucl. Instrum. Methods Phys. Res. Sect. A **479**, 117 (2002)
22. Also, see detector section in J. Brodzicka et al., Prog. Theor. Exp. Phys. 04D001 (2012)
23. S. Kurokawa, E. Kikutani, Nucl. Instrum. Methods Phys. Res. Sect. A **499**, 1 (2003) and other papers included in this volume
24. T. Abe et al., Prog. Theor. Exp. Phys. 03A001 (2013) and following articles up to 03A011
25. D.J. Lange, Nucl. Instrum. Methods Phys. Res. Sect. A **462**, 152 (2001)
26. T. Sjöstrand et al., Comput. Phys. Commun. **135**, 238 (2001)
27. R. Brun et al., GEANT, CERN Report No. DD/EE/84-1 (1984)
28. E. Nakano, Nucl. Instrum. Methods Phys. Res. Sect. A **494**, 402 (2002)
29. M. Feindt, U. Kerzel, Nucl. Instrum. Methods Phys. Res. Sect. A **559**, 190 (2006)

30. H. Nakano, Ph.D. Thesis, Tohoku University (2014). Chapter 4, unpublished. https://tohoku.repo.nii.ac.jp/?action=pages_view_main&active_action=repository_view_main_item_detail&item_id=70563&item_no=1&page_id=33&block_id=38
31. H. Albrecht et al. (ARGUS Collaboration), Phys. Lett. B **229**, 304 (1989)
32. Considering the possible change of $\mathcal{B}(\Lambda_c^+ \to pK^-\pi^+)$ in the future, we provide $\mathcal{B}(B^- \to K^-\Lambda_c^+\bar{\Lambda}_c^-)\mathcal{B}(\Lambda_c^+ \to pK^-\pi^+)^2 = (1.94 \pm 0.13 \pm 0.14) \times 10^{-6}$ and $\mathcal{B}(B^- \to \Xi_c(2930)\bar{\Lambda}_c^-)\mathcal{B}(\Xi_c(2930) \to K^-\Lambda_c^+)\mathcal{B}(\Lambda_c^+ \to pK^-\pi^+)^2 = (6.97 \pm 1.81 \pm 0.43) \times 10^{-7}$, where the first errors are statistical and the second systematic with the uncertainty on $\mathcal{B}(\Lambda_c^+ \to pK^-\pi^+)$ omitted. The 90% C.L. upper limits on $\mathcal{B}(B^- \to K^-Y(4660))\mathcal{B}(Y(4660) \to \Lambda_c^+\bar{\Lambda}_c^-)\mathcal{B}(\Lambda_c^+ \to pK^-\pi^+)^2$ and $\mathcal{B}(B^- \to K^-Y_\eta)\mathcal{B}(Y_\eta \to \Lambda_c^+\bar{\Lambda}_c^-)\mathcal{B}(\Lambda_c^+ \to pK^-\pi^+)^2$ are 4.8×10^{-7} and 8.0×10^{-7}, respectively